The assessment of prostate cancer by magnetic resonance imaging by comparing the 2D T2W and 3D T2 W

Tamara Hussein Abbas[1], Ruwaidah Abdualameer Mussttaf[1], Hussein Hasan Nsaif[2]

[1]Department of Physiology and Medical Physics, College of Medicine, Al-Nahrain University, Baghdad, Iraq
[2]Department of Surgery, College of Medicine, Al- Nahrain University, Baghdad, Iraq

ABSTRACT

Background: The prostate imaging applications, it would be particularly exciting to be able to create 3D T2-weighted MRI using SPACE. Reconstructing T2 weighted images in all three planes following the expedited capture of a single volumetric data set with the SPACE sequence may allow for significant time savings. The SPACE sequence must retain sufficient T2 contrast for the SPACE approach to be practical in a clinical context. To our knowledge, no one has previously discussed the benefits of using the SPACE sequence to detect prostate cancer.
Patient and Methods: Cross-sectional Study design, the patients with prostate cancer adults aged 40 years-80 years who diagnosed by (histopathologist) and forwarded for further investigation such as MR. The device used is MRI Siemens in Oncology Teaching Hospital, Baghdad medical city. The scanning protocols was acquired such as T1W, T2W, and FLAIR. The T2W was scanned in two ways, 3D and 2D.
Result: The prostate cancerous patient's demography was illustrated in our result. The mean age of patients was 66.2 years ± 13.28 years ranging from 31 years to 80 years. The weight of patients was 75.1 kg ± 7.07 kg. The Body Mass Index (BMI) was 24.8 Kg/m^2 ± 3.21 Kg/m^2. The comparison of the magnetic parameters of 2D and 3D of T2W images were presented in our result.
Conclusion: According to the results of our study, 3D T2 weighted acquisition for prostate imaging offers comparable tumor detection and staging performance to multiplanar conventional 2D TSE T2-weighted sequences, equivalent image quality and better relative tumor contrast than 2D TSE T2-weighted imaging.

Key words: Magnetic resonance imaging, Sampling perfection with application optimized contrast using different flip angle evolution, Nuclear magnetic resonance, Radiofrequency, Signal to noise ratio

Address for correspondence:

Tamara Hussein Abbas, Department of Physiology and Medical Physics, College of Medicine, Al- Nahrain University, Baghdad Iraq. E-mail: ttaammaarraa782@gmail.com

INTRODUCTION

Human anatomical features can be assessed and displayed using Magnetic Resonance Imaging (MRI). Nuclear Magnetic Resonance (NMR) has been used in spectroscopy for more than 50 years to identify molecules and atoms and analyze their properties. Clinical Magnetic Resonance Imaging (MRI) has been accessible since the 1980s. A plethora of diagnostic information can be obtained using Magnetic Resonance Imaging (MRI) [1]. When compared to other imaging modalities, magnetic resonance imaging's high tissue contrast is its most significant diagnostic clinical feature. The amplitude of Radio Frequency (RF), signal pulses emitted by and returning from various tissues affects the brightness of those tissues in the magnetic resonance image. The MRI technologist's choice of the right pulse sequences enables the radiologist to identify both normal tissue types and sick tissues based on changes in the MRI data [2]. In the 1950s and 1960s, chemists and physicists primarily used Nuclear Magnetic Resonance (NMR) to examine chemical compositions, configurations, and reaction processes. NMR signals from living animals were discovered by Jasper Johns, who proposed the first human applications in 1967 [3]. Lauterbur adapted a spectrometer to deliver the spatially encoded data by linear variation inside this magnetic field six year later, in 1973. He produced the first magnet resonance imaging images of two water tubes, an inhomogeneous object, using this technique (MRI). Since its infancy, clinical MRI has developed quickly. Sir Peter Mansfield published the first photographs of a living human in 1976, along with images of the hand, thorax, then head and abdomen in 1978 [4]. It was rapidly discovered that an MR system might give images with better soft tissue contrast than those obtained by the other imaging techniques after the invention of the first superconducting whole-body imager. By 1983, whole-body imaging systems that could provide high image contrast and spatial resolution had been made possible thanks to ongoing improvements in MR software and hardware [5]. The Physical Principles of the MRI: One oxygen atom and two hydrogen atoms make up the water molecule. Because it is the most prevalent element in the body, hydrogen is a useful source of energy for MRI machines. Magnetic resonance imaging is based on the movement of charged particles in an outside magnetic field, which is altered to produce a (MR) image [6].

The MRI device's component

The 3.0 Tesla Magnetic resonance imaging device seen in Figure 1, is made up of many parts that come together to form this amazing

diagnostic device. The magnet, gradient coil, Radiofrequency coil, and computer will be the main topics of discussion [7,8].

MRI physics parameters

Signal-to-Noise Ratio (SNR): The signal to noise ratio describes the relationship between the MR signal and the quantity of image noise. The standard deviation of signal strength measured outside of the anatomy and object being duplicated is known mathematically as the SNR. (i.e., a region from which no tissue signal is obtained). In MRI, a high signal to noise ratio is preferred. The SNR is affected by the following factors [9]:

- Receiver bandwidth and slice thickness.
- Field of view.
- The (image) matrix's size.
- Number of acquisitions.
- Parameters for scanning (TR, TE, flip angle).
- Strength of the magnetic field [7].

Choosing the transmission and reception coils (RF coils) Image noise is caused by a variety of factors, including:

- Imperfections in the MR system, including such as magnetic heterogeneities, thermal noise from RF coils, and signal amplifier nonlinearity.
- Factors connected with image processing.
- Patient-related factors caused by movement or respiratory motion.

To start, it's necessary to define a few visual notions. Pixels and image components combine to form a digital MR image. A two-dimensional grid with rows and columns is known as a matrix. Each pixel on the grid is represented by a square, and each square is assigned a signal strength-related integer. A voxel, a three-dimensional volume element, is represented by each pixel in an MR image. The size of the voxels in an MR picture determines its resolution [10].

METHODS

This was a cross-sectional study conducted in the Oncology Teaching Hospital, Baghdad Medical City, Radiology Department, MRI unit from November 2022 to May 2023. This study involved thirty histopathologist and forwarded for further investigation such as MRI to produce the MR images

by using two MRI sequences (2D T1W TSE, 3DT2W TSE) for the prostate cancer. In order to determine the patients' Body Mass Index (BMI), the patients' height and weight were recorded [11].

To determine the impact of weight on the quality of the MRI image, we measure the patient's weight. The patients' combined weight was 75.1 kg ± 7.07 kg. The BMI was 24.8 Kg/m^2 ± 3.21 Kg/m^2, or body mass index.

The use of a pelvic coil in an 8-element staggered array sensitivity-encoding 1.5 Tesla (MRI) system (Achieve, Siemens medical system) was made (SENSE). The ring is one size 80 cm. The computer program for MRI (Achieve application, 2005).

Inclusion criteria

- Patient's prostate cancer
- Patients with other cancerous types.
- Patients who received chemotherapy.

Exclusion criteria

- Patients with other cancerous types.
- Patients who received chemotherapy.

Statistical analyses

Analyses were performed by using IBM SPSS (statistical package of Statistical Packages for Social Sciences Statistics) version 25.0 (IBM Corp., Armonk, NY, USA). Data were presented in simple measures of percentage, mean, standard deviation. The significance of the difference of different means (quantitative data) was tested using Students-test for the difference between two independent means or the Paired-test for a difference of paired observations (or two dependent means). Statistical significance was considered whenever the p-value was equal or less than 0.05.

RESULTS AND DISCUSSION

The prostate cancerous patient's demography was illustrated in Table 1. The mean age of patients was 66.2 years ± 13.28 years ranging from 31 years to 80 years. The weight of patients was 75.1 kg ± 7.07 kg. The Body Mass Index was 24.8 Kg/m^2 ± 3.21 Kg/m^2.

Two and three-dimensional T2-weighted

The comparison of the magnetic parameters of 2D and 3D of T2W images were presented in Table 2. The statistical analysis
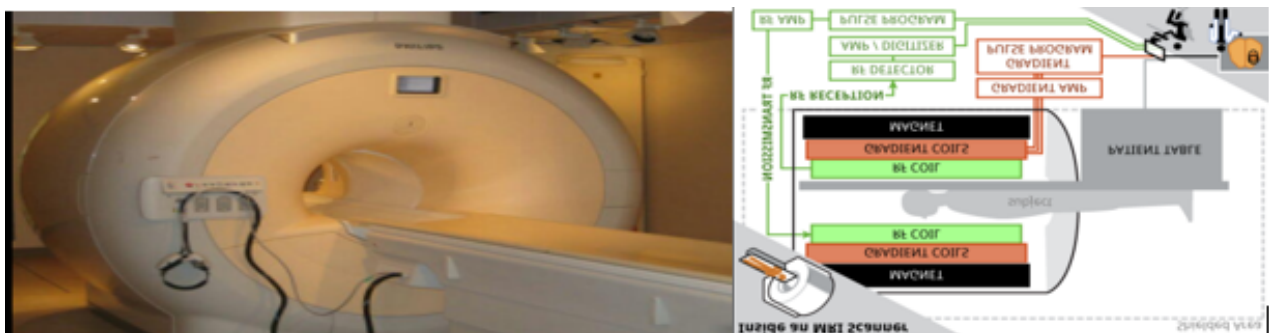

Fig. 1. Displays a 3.0 Tesla MRI apparatus and a diagram of its main components [8].

Tab. 1. Demographic results of the patients

Demography	
Age (years)	66.2 ± 13.281 (31 − 80)
Weight (kg)	75.1 ± 7.078
BMI	24.84 ± 3.21

Tab. 2. The comparison of the magnetic parameters of 2D and 3D T2W images

Parameters	2D T2-Weighted	3D T2-Weighted	*p*-value
TR	2870 ± 794.49	93.12 ± 0.323	<0.00001*
TE	72.1 ± 10.08	1360 ± 206.559	0.000104*
CNR	14.047 ± 1.91	7.36 ± 1.615	0.3897
SNR	63.29 ± 16.55	55.472 ± 6.165	0.69292
SNR max	168.2 ± 80.694	52.6 ± 14.135	0.3576
SNR min	101.1 ± 25.124	19.2 ± 3.63655219	0.28381
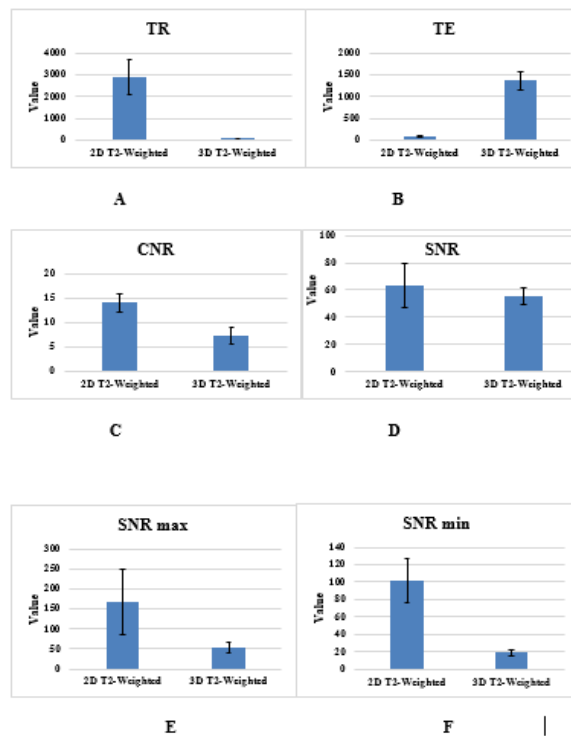
Fig. 2. (A): A comparison of the TR's 2D T2W and 3DT2W. (B): A comparison of the TE's 2D T2W and 3D T2W. (C): A comparison of the CNR's 2D T2W and 3D T2W.(D): Comparison of the mean SNR for the 2D T2W and 3DT 2W.(E): Comparison of the greatest SNR for the 2D T2W and the 3D T2W. (F): Comparison of the minimal SNR for the 2D T2W and the 3D T2W.

shows that there is a significant difference between the 2D T2W parameters for the repetition time (TR) higher than the 3D T2W, as shown in Figure 2 A. The 3D T2W shows significantly higher values of the Time to Echo (TE) than the 2D T2W, as shown in Figure 2 B. The 2D T2W shows higher values of Contrast to Noise Ratio (CNR) other than the 3D T2W with no significant difference, as shown in Figure 2 C. While the mean, maximum and minimum values of the Signal-to-Noise (SNR) show no significant difference between the two and three dimensions of T2W. The mean, minimum, and maximum values of 2D T2W were higher than the 3D T2W, as shown in figures 2 D-2F respectively.

The study population exhibited a mean age of 66.2 years with a standard deviation of 13.28 years, and a range spanning from 31 years to 80 years. The average weight of the patients was 75.1 kg, accompanied by a standard deviation of 7.07 kg. The Body Mass Index (BMI) of the participants was recorded at 24.8 kg/m², with a standard deviation of 3.21 kg/m².

The statistical analysis revealed significant differences in the Two-Dimensional (2D) T2-Weighted (T2W) parameters, specifically in terms of Repetition Time (T_R), wherein higher values were observed in 3D T2W. Furthermore, the Time to Echo (TE) values were significantly higher in 3D T2W compared to 2D T2W. In contrast, the Contrast-To-Noise Ratio (CNR) values were higher in 2D T2W compared to 3D T2W, but the difference was not statistically significant. However, no significant differences were found in the mean, maximum, and minimum values of Signal to Noise Ratio (SNR) between the two and three dimensions of T2W. Additionally, the mean, minimum, and maximum values of 2D T2W were higher than those of 3D T2W. The image scanning acquisition time for 2D T2W was 15 minutes, while the scanning time for 3D T2W was 10 minutes.

The confidence Interval (CI) analysis for both the 2D T2-weighted Turbo Spin Echo (TSE) and 3D T2-weighted TSE imaging protocols were presented in Table 2. The comparison between these protocols revealed no statistically significant differences in terms of Positive Predictive Value (PPV), Negative Predictive Value (NPV), and accuracy for the diagnosis and detection of

prostate cancer. However, the results indicated that the 3D T2W TSE protocol had significantly higher sensitivity compared to the 2D T2W TSE protocol. Conversely, the 2D T2W TSE protocol demonstrated a specificity significantly different from that of the 3D T2W TSE protocol.

CONCLUSION

We conclude that using 3D T2 weighted acquisition for prostate imaging saved us a significant amount of time compared to multiplanar conventional 2D TSE T2-weighted sequences, while providing equivalent tumor detection and staging, image quality, and better relative tumor contrast than 2D TSE T2-weighted imaging.

REFERENCES

1. Mitchell J, Webber JB, Strange JH. Nuclear magnetic resonance cryoporometry. Phys Rep. 2008; 461:1-36.

2. Grover VP, Tognarelli JM, Crossey MM, Cox IJ, Taylor-Robinson SD et al. Magnetic resonance imaging: principles and techniques: lessons for clinicians. J Clin Exp Hepatol. 2015; 5:246-55.

3. Geva T. Magnetic resonance imaging: historical perspective. J Cardiovasc Magn Reson. 2006; 8:573-80.

4. Katti G, Ara SA, Shireen A. Magnetic resonance imaging (MRI)–A review. Int J Dent Clin. 2011; 3:65-70.

5. Low RN, Barone RM, Rousset P. Peritoneal MRI in patients undergoing cytoreductive surgery and HIPEC: history, clinical applications, and implementation. Eur J Surg Oncol. 2021; 47:65-74.

6. Feng L. Golden-angle radial MRI: basics, advances, and applications. Journal of Magnetic Resonance Imaging. 2022; 56:45-62.

7. Currie S, Hoggard N, Craven IJ, Hadjivassiliou M, Wilkinson ID. Understanding MRI: basic MR physics for physicians. Postgrad Med J. 2013;89(1050):209-23.

8. Sadeghi D, Shoeibi A, Ghassemi N, Moridian P, Khadem A, et al. An overview of artificial intelligence techniques for diagnosis of Schizophrenia based on magnetic resonance imaging modalities: Methods, challenges, and future works. Comput. Biol Med. 2022:105554.

9. Koay CG, Basser PJ. Analytically exact correction scheme for signal extraction from noisy magnitude MR signals. J Magn Reson. 2006; 179:317-22.

10. De Zanche N, Barmet C, Nordmeyer-Massner JA, Pruessmann KP. NMR probes for measuring magnetic fields and field dynamics in MR systems. Magnetic Resonance in Medicine: *Off J Int Soc Magn Reson Med.,* 2008; 60:176-86.

11. Milano MT, Grimm J, Niemierko A, Soltys SG, Moiseenko V, et al. Single- and multifraction stereotactic radiosurgery dose/volume tolerances of the brain. Int J Radiat Oncol Biol Phys. 2021; 110:68-86.